Design of the low energy beam transport line for the China spallation neutron source

LI Jin-Hai(李金海) OUYANG Hua-Fu(欧阳华甫) FU Shi-Nian(傅世年)
ZHANG Hua-Shun(张华顺) HE Wei(何伟)

(Institute of High Energy Physics, CAS, Beijing 100049, China)

Abstract The design of the China Spallation Neutron Source (CSNS) low-energy beam transport (LEBT) line, which locates between the ion source and the radio-frequency quadrupole (RFQ), has been completed with the TRACE3D code. The design aims at perfect matching, primary chopping, a small emittance growth and sufficient space for beam diagnostics. The line consists of three solenoids, three vacuum chambers, two steering magnets and a pre-chopper. The total length of LEBT is about 1.74 m. This LEBT is designed to transfer 20 mA of H-pulsed beam from the ion source to the RFQ. An induction cavity is adopted as the pre-chopper. The electrostatic octupole steerer is discussed as a candidate. A four-quadrant aperture for beam scraping and beam position monitoring is designed.

Key words CSNS, LEBT, chopper, steerer, space charge

PACS 29.27.-a, 29.27.Eg

1 Introduction

The CSNS accelerator complex consists of an 81 MeV LINAC and a 1.6 GeV Rapid Cycling Synchrotron (RCS). In phase I construction, as an injector of the RCS, the LINAC consists of an H-ion source, a LEBT, a 3 MeV RFQ, a MEBT and an 81 MeV drift-tube linac (DTL). The ion source, which is basically a copy of the ISIS Penning source[1—3], will operate at 1.25% duty factor (500 μs, 25 Hz). This paper discusses the design of the LEBT.

2 The arrangement of the LEBT

The theory and method of the LEBT match had been discussed in the reference[4, 5]. To obtain a perfect match, three solenoids will be arranged in the LEBT. Besides the solenoids, there are still three vacuum chambers, two steering magnets and one pre-chopper, as shown in Fig. 1. An ion source test stand will be firstly constructed as the R&D of ion source.

In order to obtain the parameters of the beam from the ion source, a beam diagnostic line following the ion source is arranged. The test stand will be constructed structurally similar to the ISIS ion source test stand[3]. The distance between the ion source accelerator gap and the emittance scanner is designed to be about 600—700 mm both for the test stand and the LEBT, in order to keep the comparability of the measured beam parameter. Due to the limited space, only one solenoid is arranged between the ion source accelerator gap and the emittance scanner installed in the second vacuum chamber in the LEBT. According to the beam dynamics calculation result, the beam waist is formed at the upstream of the drift space between the first and the second solenoid as shown in Fig. 2. Because the smaller the beam diameter in the pre-chopper, the better, the pre-chopper is placed upstream, and the advantage of this arrangement is that any change of the beam parameters induced by the pre-chopper can be measured in the vacuum chamber.

3 The beam dynamics calculation

Before the beam dynamics calculation, the Twiss parameters and the emittances at the LEBT entrance should be given first. Two sets of the data of the experiments, one set from the standard geometry and another set from the Pierce geometry with buffer gas Kr, had been obtained from the ISIS/ISDR[3]. As the emittance scanner on the ISDR is installed 629 mm downstream the acceleration gap, the Twiss parame-

Received 22 May 2007

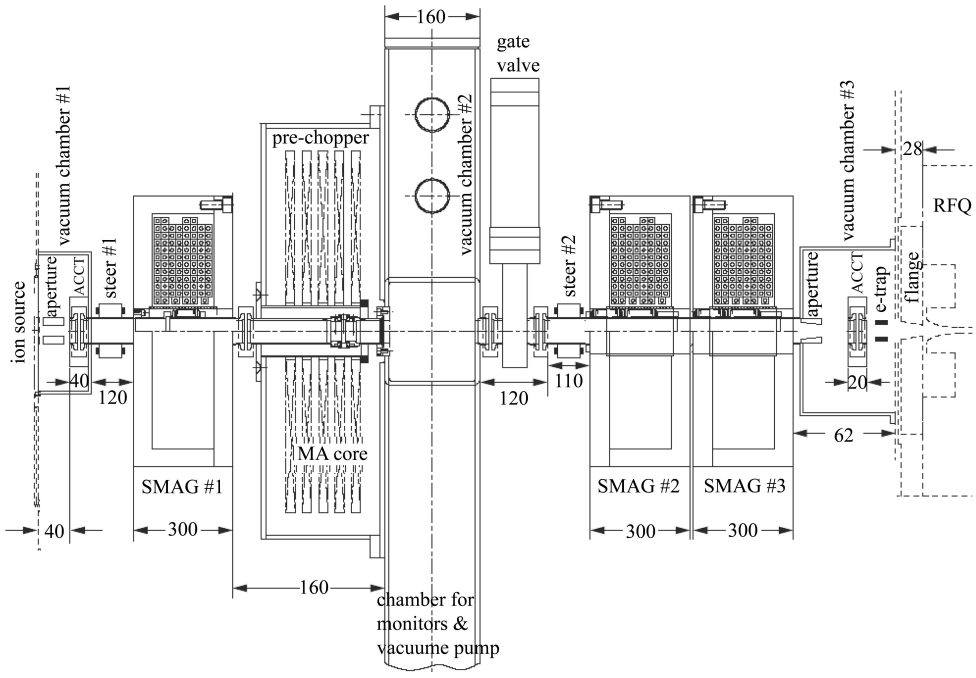

Fig. 1. The arrangement of the LEBT.

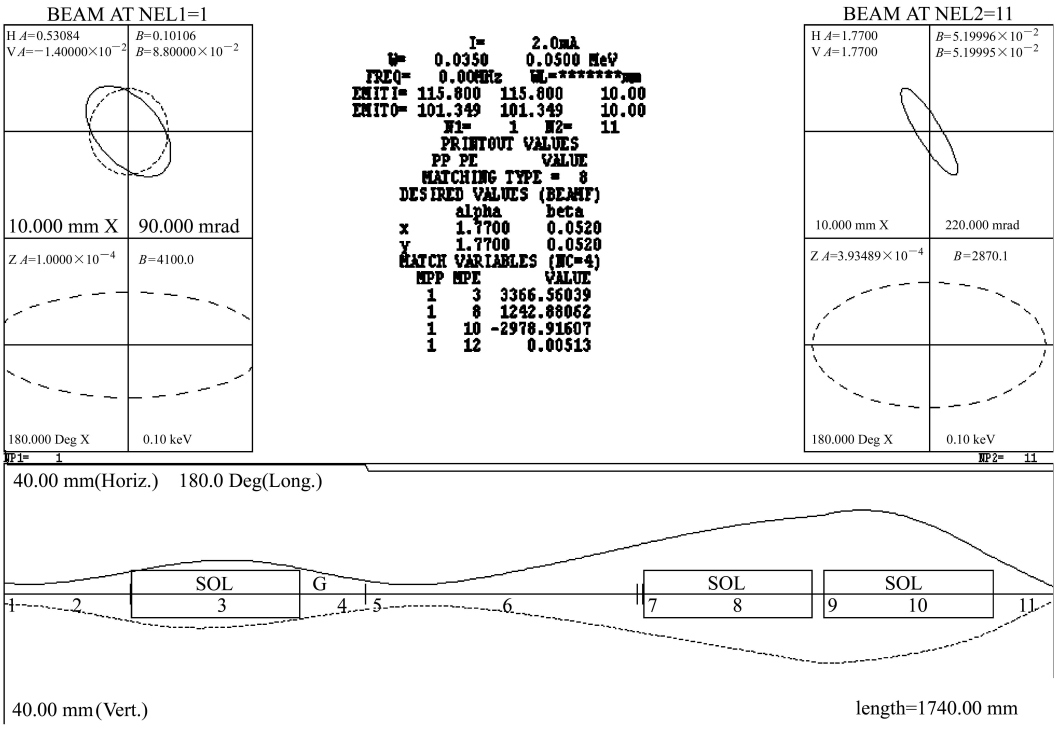

Fig. 2. The beam match result.

ters at the LEBT entrance are obtained by tracing the beam back to the accelerator gap. The got Twiss parameters at the LEBT entrance are $(\alpha,\beta)_x$= (0.53084, 0.10106), $(\alpha,\beta)_y$ = (−0.014, 0.088), and $(\alpha,\beta)_x$ = (−0.208, 0.246), $(\alpha,\beta)_y$ = (−0.904, 0.429). In the calculations, the initial emittance is supposed to be equal in the vertical and horizontal plans with $\varepsilon_{\text{Rms-Norm}}$ = 0.2 mm·mrad or $\varepsilon_{\text{Rms-Norm}}$ = 0.4 mm·mrad. Because the Twiss parameters of the beam from ISIS are for the beam energy of 35 keV, a RF gap is placed at the LEBT entrance in order to increase the beam energy to 45 kV, and another RF gap is used as pre-chopper to increase the beam energy to 50 kV.

In the calculations, 90% space charge neutralization is supposed[4]. The space charge force effect increases the complexity of the LEBT match especially for the case of the rotationally asymmetric beam extracted from the Penning source. The space charge induces not only the complex beam couple[5, 6] but also the effect of pulsed beam repeat frequency according to the simulation by TRACE3D. The reason for the frequency effect is that the space charge force is calculated by the formula[1)] for TRACE3D:

$$\begin{aligned} E_x &= \frac{3I\lambda}{4\pi\varepsilon_0 c\gamma^2}\frac{1-f}{r_x(r_x+r_y)r_z}x\,,\\ E_y &= \frac{3I\lambda}{4\pi\varepsilon_0 c\gamma^2}\frac{1-f}{r_y(r_x+r_y)r_z}y\,,\\ E_z &= \frac{3I\lambda}{4\pi\varepsilon_0 c}\frac{f}{r_x r_y r_z}z\,,\\ f &= \frac{p\ln(p+\sqrt{p^2-1})}{(p^2-1)^{3/2}}-\frac{1}{p^2-1},\quad p\equiv\frac{\gamma r_z}{\sqrt{r_x r_y}}\,. \end{aligned} \tag{1}$$

where I is for the beam current, λ for the length of the pulsed beam, ε_0 for the dielectric constant, γ and c for the relativistic factor and light velocity, r_x, r_y and r_z for the beam envelopes, x, y and z for the particle position. According to Eq. (1), the space charge force is related to r_z, which is related to the pulsed beam repeat frequency. However, since the LEBT beam has the DC character, the space charge force shouldn't be affected by the frequency. If the half phase width of the longitudinal phase ellipse is set to 180° as shown in Fig. 2, the pulsed beam can be seen as a DC beam. And then, the frequency influence is small, and the simulation result is believable. Because the frequency can't be set zero for the code TRACE3D, 25 Hz is adopted.

The theory, method and result of the chopping had been given in the reference[7—10]. The simulation showed that the energy acceptance $\Delta W/W$ of the CSNS RFQ is about ±20%, which can be used for chopping. So, if the waveform of the chopper is bipolar, the beam energy can be 45 keV before the pre-chopper, because the reference particle energy at the RFQ entrance is 50 keV. The detailed parameters of the pre-chopper will be listed later. The solenoid is designed according to the reference[11, 12].

There are numerous beam match results of the LEBT in theory. Here, only eight cases are calculated by TRACE3D[2)], and the results are listed in Table 1. The picture of the calculation result for one case of them is shown in Fig. 2. The Twiss parameters of the output beam are $(\alpha,\beta)_x$ = (1.77, 0.052), $(\alpha,\beta)_y$ = (1.77, 0.052) for all match results. Shown in Table 1, B_1, B_2 and B_3 are the magnetic fields of the first, second and third solenoid, respectively; $(\alpha,\beta)_x$ and $(\alpha,\beta)_y$ are the Twiss parameters of the input beam; $\varepsilon_{\rm i}$ is the input beam emittance and $\varepsilon_{\rm f}$ the output beam emittance. The "cross" means that there is a beam waist between the second and the third solenoid, and the "parallel" means without beam waist. From Table 1, one can see that the sum of three solenoid fields is unequal for different cases while the total rotation angle is equal. The reason is that the energy of the beam in the first solenoid is different from that in the second and the third solenoid, so the formula of the anti-correlative match[1] is:

$$\Delta B_1 = -0.948687\Delta B_{2,3}\,. \tag{2}$$

4 The design of the pre-chopper

In order to decrease the beam loss during the RCS injection, the beam of LINAC is chopped. In phase I, the chopper is only arranged in the LEBT. The time structure of the beam is shown in Fig. 3. As shown in the figure, the beam frequency is about 1.16 MHz.

Table 1. The designed parameters.

	beam parameter 1				beam parameter 2			
total length/mm	1740				1740			
α_x	0.531				−0.208			
β_x/m	0.101				0.246			
α_y	−0.014				−0.904			
β_y/m	0.088				0.429			
	cross		parallel		cross		parallel	
B_1/Gauss	3685		3367		3336		3043	
B_2/Gauss	−4067		1243		−3911		1456	
B_3/Gauss	5620		−2979		5832		−2851	
sum of field/Gauss	5238		1631		5257		1648	
total rotation angle/(°)	135.3		45.1		135.3		45.1	
pulsed beam current/mA	20	40	20	40	20	40	20	40
$\varepsilon_{\rm i}$/(mm·mrad)	0.2	0.4	0.2	0.4	0.2	0.4	0.2	0.4
$\varepsilon_{\rm f}$/(mm·mrad)	0.21	0.42	0.21	0.42	0.21	0.42	0.21	0.42
maximum envelope/mm	24	35	26	37	27	38	28	39

1) P. M. Lapostolle, CERN report AR/Int. SG/65-15, Geneva, Switzerland, July 1965

2) K. R. Crandall, D.P. Rusthoi, TRACE3D Documentation, LA-UR-97-886, May, 1997

The parameters of the designed pre-chopper operated with ±5 kV are shown in Table 2. $B_{\rm m}$ is the maximum magnetic induction; $B_{\rm a}$ is the average of the magnetic induction and ΔT is the temperature increase of the core. The magnetic core is divided into 5 pieces as shown in Fig. 4.

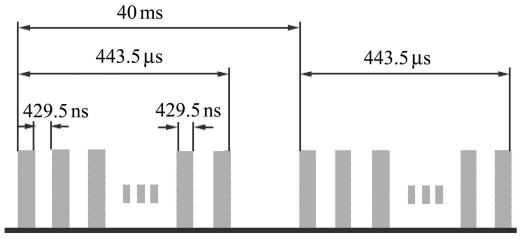

Fig. 3. The time structure of the chopped beam.

Table 2. The parameters of the pre-chopper.

$B_{\rm m}$/Gauss	3240
$B_{\rm a}$/Gauss	1220
$H_{\rm m}$/(A/m)	51.6
$I_{\rm m}$/A	14.6
L/μH	171
inner diameter/mm	90
outer diameter/mm	500
thick of core/mm	100
core loss/kW	8.1
ΔT/℃	20
weight/kg	106

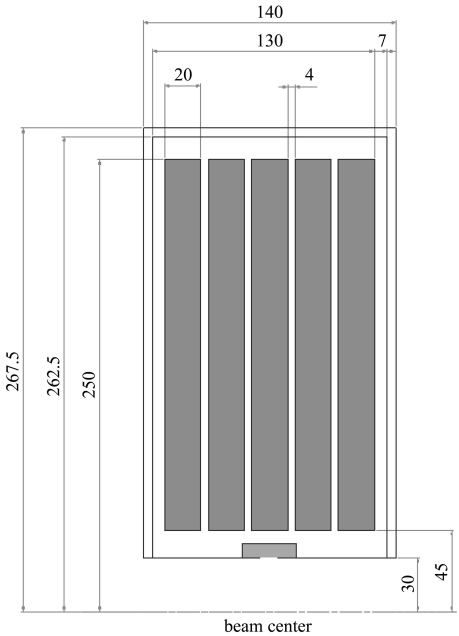

Fig. 4. The cross section of the pre-chopper.

5 The design of the steer

The steering magnet is widely used in the LEBT. As shown in Fig. 1, steering magnet is adopted in the LEBT, which is separated from the solenoid in order to avoid the possible bad effect due to the incorporation of the solenoid and the steering magnet. According to the simulation, the deviation of the magnetic field in the central area is greater than 4%. The magnetic induction of the steering magnet is generally less than 100 Gauss during operation. Because of the limited space after the third solenoid, the second steering magnet is placed before the second solenoid, which may induce the complex beam couple[6].

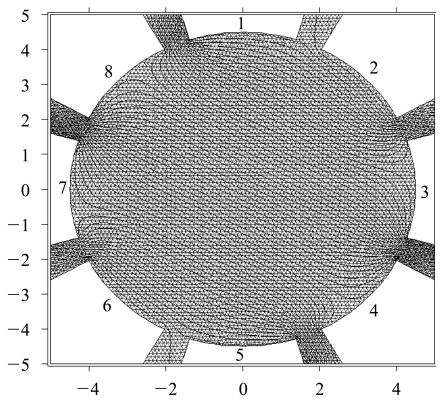

Fig. 5. The field of the electrostatic octupole steer.

In order to avoid the complex beam couple[6], the electrostatic field can be used as the steering field for the 50 keV beam. The steering field of the electrostatic octupole had been simulated by POISSON/SUPERFISH[1)]. As shown in Fig. 5, the deviation of the electrostatic field in the central area is less than 0.5%. If the beam is deflected only in y direction, the voltage ratio between the 1st and the 2nd electrode is $\sqrt{2}$. If the beam is deflected both in x and y direction at the same time, the relationship of the eight electrode voltages is:

$$\begin{aligned} V_1 &= \sqrt{2}V_Y, & V_2 &= V_X + V_Y, \\ V_3 &= \sqrt{2}V_X, & V_4 &= V_X - V_Y, \\ V_5 &= -\sqrt{2}V_Y, & V_6 &= -V_X - V_Y, \\ V_7 &= -\sqrt{2}V_X, & V_8 &= V_Y - V_X. \end{aligned} \tag{3}$$

In Eq. (3), V_X and V_Y are the deflection voltage in x and y direction. In Fig. 5, V_Y/V_X=2. The voltage control circuit of the electrostatic octupole steer is shown as Fig. 6, which satisfies Eq. (3). R_x and R_y are used to modulate V_X and V_Y, and R_1/R_2=$R_3/R_4 = \sqrt{2}-1$. In order to avoid inducing the complex beam couple and destroying the space charge neutralization by the electrostatic steerer, the electrostatic steerer must be placed at the entrance or/and the end of the LEBT. The steering field can be also used as a pre-chopper with the higher voltage. If the deflection voltages at the LEBT entrance

1) James H. Billen et al. Possion Superfish. LA-UR- 96-1834. Los Alamos, 2002

have the form of $V_Y = A\sin(\omega t)$ and $V_X = A\cos(\omega t)$, the trace of the chopped beam spot at the LEBT end should be a circle. The electrostatic steerer is just designed as a candidate of magnetic steerer because more experiments are needed to check.

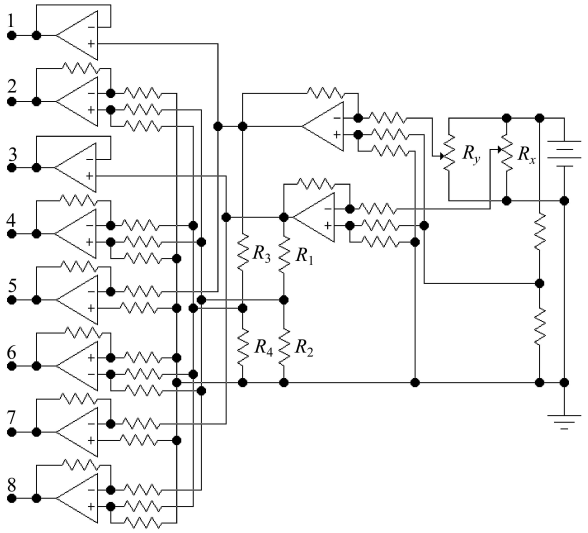

Fig. 6. The control circuit of the electrostatic steer.

6 The design of the aperture

The current and the emittance of the beam extracted from the ion source may be larger than the needed. It is necessary to scrape the unwanted beam by the aperture. In order to obtain the better beam performance, there are two apertures. One is at the front of LEBT; the other is at the end of LEBT. The inner diameter of the first aperture is very difficult to determine in advance because the Twiss parameters at the LEBT entrance beam may vary under different conditions. Its detailed size will be obtained by experiments. However, the diameter of the second aperture is fixed for the definite emittance and Twiss parameter of the RFQ entrance beam. If the second aperture is split into four quadrants as shown in Fig. 7, it can also act as the beam position monitor at the RFQ entrance.

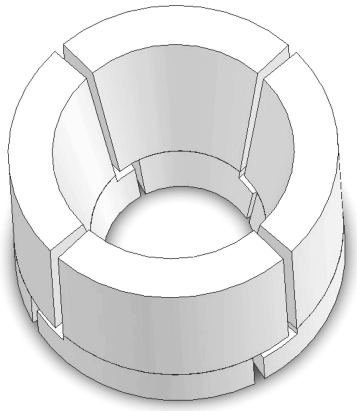

Fig. 7. The four quadrant aperture.

7 Conclusion

The physical design of the low-energy beam-transport line between the ion source and RFQ of the CSNS/LINAC has been worked out. Perfect matching in four dimensions phase space and preliminary chopping are achieved by means of three solenoids, two steering magnets, two apertures and one pre-chopper. The length of the beam line is about 1.74 m. In the beam line, sufficient space for the beam diagnostic system has been left. The design result of the pre-chopper has been given. The control circuit and the simulation of the electrostatic octupole steerer are discussed. The four quadrants aperture for monitoring the beam position is designed.

References

1 Thomason J W G, Sidlow R. EPAC 2000. 1625—1627
2 Faircloth D C, Sidlow R , Whitehead M O et al. PAC 2005. 1910—1912
3 Thomason J W G, Faircloth D C, Sidlow R et al. EPAC 2004. 1458
4 Ferdinand Robin, Sherman Joseph, Stevens Ralph R et al. PAC 1997. 2723—2725
5 LI J H, TANG J Y. Nuclear Instruments and Methods in Physics Research Section A, 2007, **574**(2): 221—225
6 LI J H, TANG J Y, OUYANG H F et al. Nuclear Instruments and Methods in Physics Research Section A (has been submitted)
7 Ohmori C, Kanazawa M, Takagi A et al. Nuclear Instruments and Methods in Physics Research A, 2004, **526**: 215—221
8 Chou W, Mori Y, Muto M et al. PAC 1999. 565—567
9 Mori Y, Muto M, Ohmori C et al. EPAC 2000. 2468—2470
10 Mori Y, Muto M, Ohmori C et al. TPAC 2001. 4056—4058
11 Bailey C P. EPAC 1998. 1162—1164
12 Jolly S, Pozimski J, Faircloth D et al. EPAC 2006. 1714—1716